

Video-Based Detection of Generalized Tonic-Clonic Seizures Using Deep Learning

Yonghua Yang, Rani A. Sarkis, Rima El Atrache , Tobias Loddenkemper, and Christian Meisel 

Abstract—Timely detection of seizures is crucial to implement optimal interventions, and may help reduce the risk of sudden unexpected death in epilepsy (SUDEP) in patients with generalized tonic-clonic seizures (GTCSs). While video-based automated seizure detection systems may be able to provide seizure alarms in both in-hospital and at-home settings, earlier studies have primarily employed hand-designed features for such a task. In contrast, deep learning-based approaches do not rely on prior feature selection and have demonstrated outstanding performance in many data classification tasks. Despite these advantages, neural network-based video classification has rarely been attempted for seizure detection. We here assessed the feasibility and efficacy of automated GTCSs detection from videos using deep learning. We retrospectively identified 76 GTCS videos from 37 participants who underwent long-term video-EEG monitoring (LTM) along with interictal video data from the same patients, and 10 full-night seizure-free recordings from additional patients. Using a leave-one-subject-out cross-validation approach (LOSO-CV), we evaluated the performance to detect seizures based on individual video frames (convolutional neural networks, CNNs) or video sequences [CNN+long short-term memory (LSTM) networks]. CNN+LSTM networks based on video sequences outperformed GTCS detection based on individual frames yielding a mean sensitivity of 88% and mean specificity of 92% across patients. The average detection latency after presumed clinical seizure onset was 22 seconds. Detection performance increased as a function of training dataset size. Collectively, we demonstrated that

automated video-based GTCS detection with deep learning is feasible and efficacious. Deep learning-based methods may be able to overcome some limitations associated with traditional approaches using hand-crafted features, serve as a benchmark for future methods and analyses, and improve further with larger datasets.

Index Terms—Epilepsy, seizure detection, video.

I. INTRODUCTION

RELIABLE assessments of seizure frequency are essential for epilepsy diagnosis, syndrome evaluation, treatment selection, and prognosis. Similarly, timely seizure alerts are also crucial to prevent potential complications from seizures such as secondary injuries, and to initiate treatment to stop a seizure. In patients with generalized tonic-clonic seizures (GTCSs), timely detection of seizures may be particularly important in order to limit the risk of sudden unexpected death in epilepsy (SUDEP) [1]. Video-EEG monitoring performed in specialized epilepsy monitoring units (EMUs) is the gold-standard in detecting and classifying epileptic seizures. However, this technique is also time-and labor-consuming and only available at specialized centers. Automated methods to detect seizures, in particular GTCSs, may help improve patient monitoring and reduce the time and labor involved in screening and evaluating long-term video-EEG data in specialized EMU settings. Apart from video or EEG, other modalities, including accelerometry, electrodermal activity and electromyogram, have been explored for seizure detection [28]–[31], [38], [39]. Detection of seizures using video only, however, remains desirable since it does not require contact with the patient, and can be employed relatively easily, including the use of potentially already existing video hardware in many settings.

The potential benefits associated with video-based seizure detection have spurred research efforts in this direction for more than a decade [33]. Initial studies have primarily employed hand-designed features based on motion-strength, motion-trajectory [2]–[4] or average differential luminance signals [5], [6] in video segments in order to develop automated seizure detection systems. These approaches focused mainly on motor signs, but performance was sometimes limited by the inability of algorithms to generalize and provide good performance results in the setting of changing luminance or occlusion of the patient, such as patients covered by a blanket [7]. Deep learning has led to performance improvements in many fields. A recent systematic review, for example, revealed that deep learning-based EEG

Manuscript received June 24, 2020; revised October 6, 2020 and December 17, 2020; accepted December 28, 2020. Date of publication January 6, 2021; date of current version August 5, 2021. This work was supported by the Epilepsy Research Fund. The work of Yonghua Yang was supported by Scientific & Technological Fundation of Shaanxi Province under Grant 2018SF-096. The work of Christian Meisel was supported by the NARSAD Young Investigator Grant by the Brain & Behavior Research Foundation. (*Corresponding author: Christian Meisel.*)

Yonghua Yang is with the Division of Epilepsy and Clinical Neurophysiology, Department of Neurology, Boston Children's Hospital, Harvard Medical School, Boston, MA 02115 USA, and also with the Department of Pediatrics, Hospital of Xi'an Jiaotong University, Xi'an 710061, China (e-mail: yyhflower@126.com).

Rani A. Sarkis is with the Edward B. Bromfield Epilepsy Program, Brigham and Women's Hospital, Boston, MA 02115 USA (e-mail: rsarkis@bwh.harvard.edu).

Rima El Atrache and Tobias Loddenkemper are with the Division of Epilepsy and Clinical Neurophysiology, Department of Neurology, Boston Children's Hospital, Harvard Medical School, Boston, MA 02115 USA (e-mail: rima.elatrache@childrens.harvard.edu; tobias.loddenkemper@childrens.harvard.edu).

Christian Meisel is with the Department of Neurology, Charité-Universitätsmedizin Berlin, 10117 Berlin, Germany, and also with the Berlin Institute of Health, 10178 Berlin, Germany (e-mail: christian@meisel.de).

Digital Object Identifier 10.1109/JBHI.2021.3049649

analysis gained a 5.4% median accuracy increase over traditional baselines across all relevant studies [27]. These improvements also include computer vision, which may help overcome some of the limitations associated with hand-crafted features. Compared to traditional machine learning approaches, deep learning techniques are capable of learning underlying spatio-temporal feature representations from training data without the need for hand-designed features [8]. In epilepsy, for example, the use of convolutional neural networks (CNNs) has previously been applied to seizure detection relying on a single video frame approach [9]. Deep learning applied to video sequences has also been used for motion and facial analysis in patients with mesial temporal and extra-temporal lobe epilepsy [10]–[12]. Deep learning-based techniques are therefore a promising approach for detecting GTCSs from video with high sensitivity and specificity. They may also help overcome the limitations of more traditional machine learning methods and the need of hand-crafted feature sets. Despite these advantages in performance and methodology, deep learning-based video classification has rarely been attempted for seizure detection. We here assessed the feasibility and efficacy of automated GTCSs detection from videos using deep learning. Specifically, we assess the feasibility and compare the performance of a GTCS detection system based on single video frames and video sequence data using deep learning. Our work is motivated by the potential benefits of such a system to monitor patients with seizure risk in both hospital-based and home-based settings, improve seizure outcome assessment, and provide caregivers and clinicians with timely warnings, in particular for patients at risk for SUDEP.

II. MATERIALS AND METHODS

A. Video Data Collection

The video data were selected from participants undergoing long-term video-EEG monitoring (LTM) at Boston Children's Hospital. The study was approved by the Institutional Review Board at Boston Children's Hospital and written informed consent was obtained from all participants or from their parents/guardians. LTM recordings were recorded using conventional scalp EEG montages according to 10-20 electrode system. The majority of the videos were recorded by a high-definition camera (Sony SNC 550, Tokyo, Japan), which was mounted at the ceiling of the monitoring room. The cameras used in this study had a BW/RGB auto-switching function. In low light they used B/W, in bright light color. Sometimes the technician/staff in the EMU may have locked settings to B/W, if the image quality looked better. Recorded videos were sampled in AVI format with a resolution of 1080×720 or 320×240 pixels at 30 frames per second and 4096 kbps. Videos were reviewed for clinical purposes by an independent board-certified epileptologist. For further analysis, only videos were included from participants who had at least one generalized tonic-clonic seizure (GTCS) with either focal or generalized onset. Four videos of seizures had to be excluded because the patient was either off camera at the beginning of the seizure, the video was of poor quality (pixelated and shaky images), the video ended before the start of the tonic phase, or the seizure evolved into status epilepticus.

Based on these criteria, we identified 76 videos with GTCSs from 37 participants. These seizure video-EEGs were then re-reviewed independently by two epileptologists (RAS, TL) to determine electrographic and clinical seizure onset and offset, onset of the tonic phase, clinical manifestation, as well as seizure semiology. Patient data were obtained by chart review, including demographics, seizure history, and MRI findings.

Additionally, we identified ten full night seizure-free video recordings (8 hours: 10 pm-6 am) from ten additional participants, according to the LTM report verified by an independent board-certified epileptologist as well as annotations in Natus by EEG technologists and epileptologists.

B. Video Data Preprocessing

Seizure video clips were saved from clinical seizure onset to clinical seizure offset for each seizure. In one seizure the clinical onset and offset were not clear because of occlusion by a blanket, and in this case the EEG onset and offset were used. Interictal videos were obtained from the same participants and included seizure-free periods that occurred at least 10 seconds prior to a seizure and at least 15 minutes after a previous seizure. All interictal, ictal and night video clips were recorded, and then resampled as MP4 format using Camtasia (version 2019.0.7, TechSmith, Okemos, MI, USA) with whole screen mode in 480×270 pixel resolution. We limited our analysis to video data only, thus discarding the audio component of the original videos. To account for potential confounders, such as number of people in the video, we noted the number of the people in the ictal video clips in addition to the patient as applicable at each second in the ictal video.

C. Preparation of Training and Test Data

We applied a leave-one-subject-out cross-validation (LOSO-CV) approach where matched data from 36 participants were used for training, and testing was done on all of the collected video data from the remaining out-of-sample patient. For preparation of the training datasets, we first separated all video files into consecutive, non-overlapping 5-second clips. We included all ictal 5-second clips after the start of the tonic phase in a patient for training and matched them with an equal number of randomly chosen interictal 5-second clips from the same patient. This matching was performed to handle the imbalanced data during training where interictal data often outnumber ictal data by a large factor. Next, the matched data from 36 participants were used for training while testing was performed on the remaining patient's full videos (ictal, interictal). Additionally, each trained network was also applied to the ten full night recordings for inference.

D. Neural Networks and Training

We assessed detection based on two different approaches: single video frames (CNN approach) and frame sequences, i.e., taking also the temporal dynamics into account [CNN+long short-term memory (LSTM) approach]. Video frames were first resized to 224×224 pixel resolutions. Then, a CNN network for

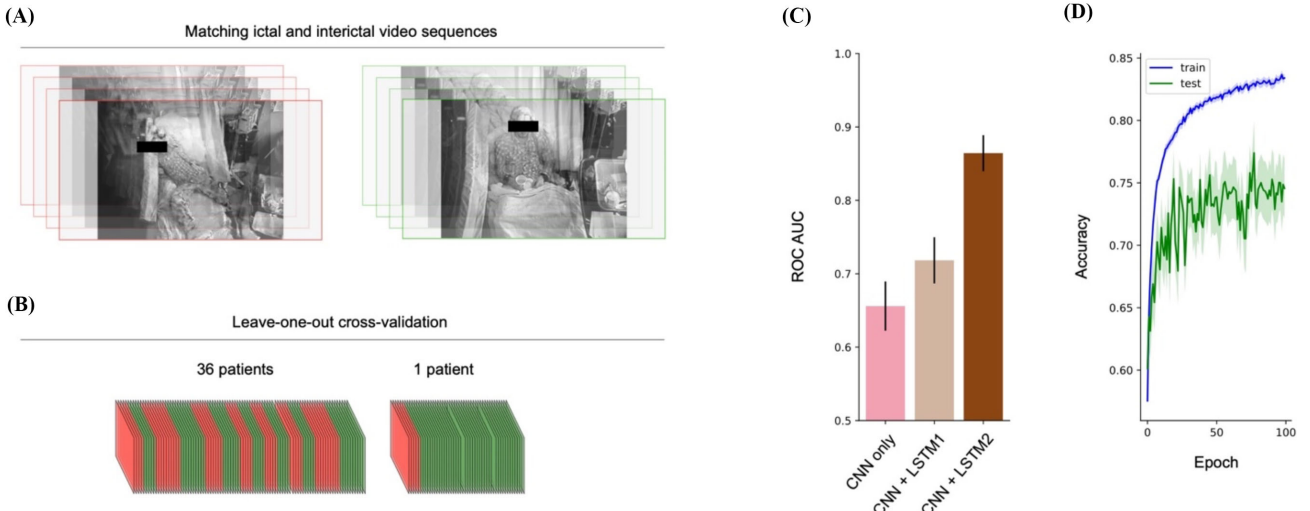


Fig. 1. Outline of data processing for automated video seizure detection. **A**, Consecutive ictal video clips of 5 seconds duration (red) were matched with the same number of interictal video clips (green) for each patient. **B**, A leave-one-out cross-validation (LOSO-CV) approach that trained on matched data from all but one patient and evaluated on the full data from the remaining patient was implemented to assess performance. **C**, Area under the ROC curve (AUC) for seizure detection based only on static video frames (CNN only) and for CNN+LSTM networks. **D**, Learning curves for CNN+LSTM2 networks. Signed consent forms authorizing publication have been obtained for all identifiable patients.

each patient in the LOSO-CV approach was trained individually using the first frame of each 5-second video clip and used for testing on the one left-out patient. Fig. 5 shows details of the CNN architecture and hyperparameters. For the CNN+LSTM approach, these trained CNN networks were then used for encoding of individual video frames, excluding the CNN top layers. The output of the CNNs, a 100-element long vector, was subsequently fed to a stacked LSTM architecture, to encode the temporal sequence of these outputs. For each 5-second video clip, LSTMs were thus fed with a tensor of 150 frames (at 30 Hz) by 100. LSTMs are specifically designed architectures for learning underlying representations in time series data. We tested two LSTM architectures with varying numbers of hidden units; the output of the hidden recurrent layer is finally fed into a densely connected layer with a sigmoid activation function. To limit networks from overfitting, regularization methods (dropout) were incorporated and training was performed on matched data where both classes appeared equally often (Fig. 1 A, B). CNN and CNN+LSTM network training was done by optimizing the binary cross-entropy loss using the Adam optimizer. Analyses were performed with in-house written code in Python (version 2.7) and Keras (Tensorflow backend).

E. Performance Metrics

We applied a LOSO-CV approach where matched ictal/interictal video clips from 36 participants were used for training, and testing was done on the full data of the one remaining out-of-sample patient (Fig. 1 A, B). The detection method provided a value between 0 and 1 for each 5-second interval (based on video or first frame in this interval). We assessed detection performance in terms of area under the ROC curve (AUC), sensitivity, and specificity. AUC was calculated for all

5-second segments after the annotated start of the tonic phase and the interictal data. For the following metrics, a 5-second interval was defined as ictal if the detection method predicted a value of equal or larger than 0.5 for this interval and as interictal otherwise. Sensitivity was then defined as the fraction of seizures correctly detected, i.e., during which at least one 5-second epoch was classified as ictal. Specificity was defined as the fraction of true negative 5-second epochs during interictal data. We also assessed latency of detection after the clinically annotated start of the seizure, defined as the time difference of the first 5-second segment classified as ictal to the clinically annotated start of the seizure. The false detection rate (FDR) was assessed in ten additional full-night, seizure-free recordings where it was determined as the number of false positive alarms per night (8 hours; 10 pm to 6 am) and allowed a 10-minute buffer before a new, consecutive alarm could be sounded.

III. RESULTS

A. Demographics and Clinical Characteristics of the Enrolled Participants

Our training dataset consisted of 76 GTCSs from 37 participants (14.2 ± 2.5 years, mean \pm standard deviation (SD), 54.1% females, Table I). Demographic characteristics in detail are shown in Table III. The mean duration of ictal video data per patient was 2.73 ± 0.33 minutes. About half of the seizures occurred during sleep (39/76). The proportion of focal to bilateral tonic-clonic seizure was 77.6% (59/76). The seizure characteristics are shown in Table IV. For each patient, we also considered interictal videos (mean duration 15.35 ± 3.75 minutes) during which participants were either

TABLE I
SUMMARIZED CHARCTERISTICS OF GTCS PATIENTS (N = 37)

Demographic Characteristics	
Female n (%)	20 (54.1)
Age at EEG (years, mean \pm SD)	14.2 \pm 2.5
Age at First Seizure (years, mean \pm SD)	7.3 \pm 5.5
Median Seizure Frequency/30 days¹(range, IQR)	4.3 (0.0-375.0, 1.0-30.0)
Number of Seizures Enrolled (mean \pm SD)	2.0 \pm 1.1
Etiology	n (%)
Structural	16 (43.2)
Unknown	14 (37.8)
Genetic	2 (5.4)
Infectious	2 (5.4)
Immune	2 (5.4)
Metabolic	1 (2.7)
MRI Findings²	n (%)
Malformation	9 (24.3)
Tumor	6 (16.2)
Encephalomalacia	3 (8.1)
Gliosis	4 (10.8)
Volume Loss	4 (10.8)
Cyst	2 (5.4)
Inflammation	2 (5.4)
Normal	9 (24.3)
Others ³	4 (10.8)

¹If the seizure frequency is a value in a range, we took the average of the boundary values as the seizure frequency for further analysis. For one patient who had multiple unquantifiable seizures per day, we used 100 as the seizure frequency per 30 days. For two patients who had several/a few unquantifiable seizures per month, we used 3 as their seizure frequency per 30 days.

²Patients may have been represented in more than one category and numbers, therefore, numbers do not add up to 37 (100%).

³Other MRI findings include Sturge Weber syndrome, hydrocephalus, tuberous sclerosis, and cavernoma.

sleeping or awake, and engaged in baseline activities. Additionally, we also included 10 nights from 10 different participants without seizures (10.7 ± 5.0 years, mean \pm SD; 60% female). The detailed demographic characteristics are shown in Table V.

B. Performance of Individual-Frame and Video-Based GTCS Detection Systems

We first assessed seizure detection performance when only individual video frames were considered (CNN approach) and then compared it to more complex methods taking into consideration

TABLE II
COMPARISON OF FACTORS INFLUENCING DETECTION LATENCIES

Percentage	Group 1	Group 2	Odds Ratio	P value
Asleep%	0.43	0.63	0.45	0.1498
Occlusion%	0.73	0.81	1.58	0.5755
Interaction%	0.39	0.52	1.69	0.3361
Other people appearing in the videos%	0.86	0.78	0.59	0.5255
Illumination changes%	0.14	0.11	0.75	1.0000
Higher	0.43	0.59	0.52	0.2315
Resolution%				

Fisher's exact test was used for the comparisons. Group 1: detection latencies are within 10 s. Group 2: detection latencies are longer than 10 s.

also the temporal succession of video frames (CNN+LSTM approaches). Thus, the detection based on individual frames served as a baseline performance measure for comparison and benchmarking of the more complex CNN+LSTM approaches. Based on AUC, seizure detection using only individual video frames performed worst, albeit better than chance. Performance increased when CNNs were combined with LSTM networks to take the temporal succession of video frames into account (Fig. 1C). Learning curves indicated no sign of overfitting (Fig. 1D). The best performance was achieved for an LSTM network with 1000 hidden units (CNN+LSTM2) which outperformed smaller networks (CNN+LSTM1). The following results are reported for this best-performing approach, as an average over two independently trained networks for each patient. Fig. 2 shows the performance in terms of sensitivity and specificity for all 37 participants. Nine of the 76 seizures were not detected. Across participants, we report a mean sensitivity of $88 \pm 5\%$ (mean \pm standard error of the mean (s.e.m)) and mean specificity of $92 \pm 2\%$. The average seizure detection latency as measured from clinical seizure onset was 22 ± 3 seconds. As an additional estimate of specificity, the false discovery rate determined across ten additional full-night, seizure-free recordings yielded 12 ± 1 per night.

C. Possible Factors Influencing Detection Performance

To assess potential influence of appearance of other people (e.g., caregivers) in the video on the CNN+LSTM2 seizure detection, we labeled the times when one or more persons in addition to the patient appeared in the video for the first time. Fig. 3 shows the time course of seizure likelihood for all participants along with an indicator when other persons appear in the video for the first time (black vertical lines) and the start of the tonic phase (black round markers). Ten seizures were correctly detected prior to appearance of another person in the video (Fig. 3). Furthermore, two seizures were detected without any

TABLE III
GTCS PATIENT CHARACTERISTICS IN DETAIL

Patient ID	Gender	Age at EEG [years]	Age at First Seizure [years]	Seizure Frequency/30d	Etiology	MRI Findings	Number of Seizures Enrolled
1	male	16.7	11.2	0.2	structural	tumor	2
2	female	14.6	7.0	375.0	structural	infarction and encephalomalacia	6
3	female	11.3	9.6	2.0	structural	tumor	2
4	female	17	15.0	0.0	unknown	normal	1
5	male	15.9	13.4	0.3	structural	malformation	1
6	female	14.4	6.0	3.0	unknown	malformation	2
7	male	17.9	15.4	2.0	structural	tumor	1
8	female	13.5	0.0	20.0	genetic	gliosis and volume loss	1
9	male	9.9	1.5	1.0	unknown	normal	1
10	female	22.2	10.0	0.3	structural	cystic encephalomalacia and gliosis	1
11	male	9.3	7.0	1.5	unknown	malformation and cyst	2
12	female	27.4	14.0	3.0	metabolic	normal	3
13	female	5.2	5.2	7.0	infectious	inflammation	3
14	female	19.7	0.3	315.0	unknown	malformation, gliosis, and volume loss	1
15	female	11.6	10.5	7.0	structural	tumor	4
16	female	17.7	1.2	1.0	unknown	malformation	3
17	male	10.3	8.7	45.0	infectious	gliosis	1
18	male	13.3	0.5	30.0	genetic	tuberous sclerosis	2
19	female	13.8	11.0	100.0	immune	volume loss	2
20	female	13.8	8.5	4.3	unknown	normal	4
21	male	13.9	0.3	2.0	structural	malformation	3
22	male	11	1.5	85.0	unknown	normal	2
23	male	9.5	1.7	10.7	structural	tumor	2
24	male	13.1	0.5	4.3	unknown	normal	1
25	female	20.7	16.0	0.2	unknown	cavernoma	3
26	male	9.9	5.0	150.0	unknown	normal	2
27	male	14.5	13.0	10.7	structural	tumor	1
28	male	8.9	1.1	30.0	structural	encephalomalacia and volume loss	1
29	male	19.8	8.5	5.1	unknown	normal	3
30	male	12.8	1.3	4.3	structural	Sturge Weber syndrome	1
31	female	15.4	13.7	0.3	unknown	cyst	3
32	female	18.9	17.4	1.3	structural	malformation	1
33	female	17.1	13.5	0.0	structural	hydrocephalus	2
34	female	12.4	0.8	30.0	structural	malformation	3
35	male	11.1	1.0	60.0	structural	malformation	1
36	female	8.2	6.2	0.2	unknown	normal	2
37	female	13.2	11.5	0.0	immune	inflammation	2

other visible people in the videos. Collectively, these analyses and examples indicate that the algorithm did not solely use the presence of other people in the video to classify video data as a seizure.

We also analyzed other possible factors which might influence detection latencies, including wakefulness (before seizure onset), occlusion status, interaction with other people, other people appearing in the videos, resolution of the original video,

and illumination changes before or during the time of seizure detection (Table II). Sixty-four percent of seizures (49/76) were detected within 10 seconds from the start of the GTCS onsets. Compared to the seizures with longer latencies, the differences of the proportion in occlusion, illumination, other people appearing in the videos, wakefulness, resolution of the original video, and interaction with other people were not significant ($P>0.05$, Fisher's exact test).

TABLE IV
CHARACTERISTICS OF SEIZURES (76)

Seizure ID	Patient ID	Ictal Videos Duration	State of Wakefulness	ILAE Semiology	EEG location	EEG laterization
1	1	0:01:21	awake	focal to bilateral tonic-clonic	centro-parietal	right
2	1	0:00:43	awake	focal to bilateral tonic-clonic	centro-parietal	right
3	2	0:01:36	asleep	focal to bilateral tonic-clonic	central	right
4	2	0:01:07	awake	focal to bilateral tonic-clonic	central	right
5	2	0:01:15	asleep	focal to bilateral tonic-clonic	central	right
6	2	0:01:03	asleep	focal to bilateral tonic-clonic	central	right
7	2	0:01:21	asleep	focal to bilateral tonic-clonic	central	right
8	2	0:04:21	asleep	focal to bilateral tonic-clonic	central	right
9	3	0:01:34	asleep	focal to bilateral tonic-clonic	frontal	right
10	3	0:01:10	asleep	focal to bilateral tonic-clonic	frontal	right
11	4	0:01:32	awake	focal to bilateral tonic-clonic	temporal	left
12	5	0:02:05	awake	focal to bilateral tonic-clonic	frontal	right
13	6	0:01:31	awake	focal to bilateral tonic-clonic	central	left
14	6	0:01:25	awake	focal to bilateral tonic-clonic	central	left
15	7	0:01:46	awake	focal to bilateral tonic-clonic	parietal	left
16	8	0:00:53	awake	generalized tonic-clonic	generalized	generalized
17	9	0:00:24	asleep	focal to bilateral tonic-clonic	frontal	bilateral
18	10	0:01:44	asleep	focal to bilateral tonic-clonic	centro-parietal	left
19	11	0:01:18	asleep	focal to bilateral tonic-clonic	fronto-central	right
20	11	0:01:32	asleep	focal to bilateral tonic-clonic	fronto-central	right
21	12	0:01:01	awake	generalized tonic-clonic	generalized	generalized
22	12	0:00:58	asleep	generalized tonic-clonic	generalized	generalized
23	12	0:01:19	awake	generalized tonic-clonic	generalized	generalized
24	13	0:00:23	awake	generalized tonic-clonic	generalized	generalized
25	13	0:00:19	awake	generalized tonic-clonic	generalized	generalized
26	13	0:00:26	asleep	generalized tonic-clonic	generalized	generalized
27	14	0:00:30	awake	generalized tonic-clonic	generalized	generalized
28	15	0:02:33	asleep	generalized tonic-clonic	generalized	generalized
29	15	0:01:07	awake	generalized tonic-clonic	generalized	generalized
30	15	0:01:30	asleep	generalized tonic-clonic	generalized	generalized
31	15	0:02:04	asleep	generalized tonic-clonic	generalized	generalized
32	16	0:01:02	awake	generalized tonic-clonic	generalized	generalized
33	16	0:00:50	awake	generalized tonic-clonic	generalized	generalized
34	16	0:01:07	awake	generalized tonic-clonic	generalized	generalized
35	17	0:00:54	awake	focal to bilateral tonic-clonic	centro-temporal	right
36	18	0:00:22	awake	focal to bilateral tonic-clonic	parasagittal	right
37	18	0:00:30	awake	focal to bilateral tonic-clonic	parasagittal	right
38	19	0:00:58	awake	focal to bilateral tonic-clonic	frontal temporal	left
39	19	0:01:04	asleep	focal to bilateral tonic-clonic	frontal temporal	left
40	20	0:01:20	asleep	focal to bilateral tonic-clonic	central	midline
41	20	0:01:32	asleep	focal to bilateral tonic-clonic	central	midline

D. Performance Improvement With Larger Training Set Size

Deep learning may benefit from large datasets that afford learning of the underlying data representations while also providing sufficient variability to permit generalization to novel

data. To determine the relationship between seizure detection performance and size of the training dataset, we evaluated performance based on different amounts of training data. For this purpose, instead of training on all 36 patients in a leave-one-subject-out approach, as described above, we systematically

TABLE IV
CONTINUED

42	20	0:01:17	asleep	focal to bilateral tonic-clonic	central	midline
43	20	0:01:20	asleep	focal to bilateral tonic-clonic	central	midline
44	21	0:01:02	asleep	focal to bilateral tonic-clonic	parietal	left
45	21	0:02:00	asleep	focal to bilateral tonic-clonic	parietal	left
46	21	0:01:36	asleep	focal to bilateral tonic-clonic	parietal	left
47	22	0:01:50	awake	focal to bilateral tonic-clonic	temporal	left
48	22	0:01:37	awake	focal to bilateral tonic-clonic	temporal	left
49	23	0:01:12	asleep	focal to bilateral tonic-clonic	posterior/parasagittal	right
50	23	0:01:33	asleep	focal to bilateral tonic-clonic	posterior/parasagittal	right
51	24	0:01:01	awake	focal to bilateral tonic-clonic	frontal	bilateral
52	25	0:01:29	asleep	focal to bilateral tonic-clonic	temporo-occipital	left
53	25	0:01:22	asleep	focal to bilateral tonic-clonic	temporo-occipital	left
54	25	0:01:32	asleep	focal to bilateral tonic-clonic	temporo-occipital	left
55	26	0:00:47	asleep	focal to bilateral tonic-clonic	central	left/midline
56	26	0:00:32	asleep	generalized tonic-clonic	parasagittal	bilateral/midline
57	27	0:01:34	awake	focal to bilateral tonic-clonic	temporal	right
58	28	0:01:13	asleep	focal to bilateral tonic-clonic	posterior	right
59	29	0:01:15	asleep	focal to bilateral tonic-clonic	frontal	right
60	29	0:01:04	asleep	focal to bilateral tonic-clonic	frontal	bilateral
61	29	0:00:46	asleep	focal to bilateral tonic-clonic	frontal	bilateral
62	30	0:03:11	awake	focal to bilateral tonic-clonic	temporal occipital	left
63	31	0:01:07	awake	generalized tonic-clonic	generalized	generalized
64	31	0:01:22	awake	focal to bilateral tonic-clonic	posterior temporal	left
65	31	0:01:46	awake	focal to bilateral tonic-clonic	temporal	right
66	32	0:01:50	awake	focal to bilateral tonic-clonic	temporal	right
67	33	0:03:52	awake	focal to bilateral tonic-clonic	Parietal	right
68	33	0:02:01	awake	focal to bilateral tonic-clonic	Parietal	right
69	34	0:01:32	awake	focal to bilateral tonic-clonic	temporal	right
70	34	0:01:14	awake	focal to bilateral tonic-clonic	posterior temporal	right
71	34	0:01:37	awake	focal to bilateral tonic-clonic	posterior temporal	right
72	35	0:00:30	awake	focal to bilateral tonic-clonic	parietal/posterior temporal	left
73	36	0:01:08	asleep	focal to bilateral tonic-clonic	centro-temporal	right
74	36	0:01:44	asleep	focal to bilateral tonic-clonic	centro-temporal	right
75	37	0:01:26	awake	focal to bilateral tonic-clonic	temporal	left
76	37	0:01:57	asleep	focal to bilateral tonic-clonic	temporo-parietal	right

reduced the amount of training data by considering only a smaller number of patients ($n = 5$ or $n = 20$ patients) for training. Performance, assessed by AUC ROC values, increased with more patients used for training (Fig. 4). This may indicate further improvement of seizure detection performance with larger datasets in the future.

IV. DISCUSSION

Deep learning has rarely been attempted for video-based seizure detection. In this study, we used deep learning to 1) evaluate GTCS detection on videos, 2) compare approaches based on individual frames vs. videos, 3) determine the role of possible factors influencing detection performance, and 4)

determine the algorithm performance's dependence on training data size. Our results indicate that video-based GTCSs detection using deep learning without the need for feature-designing is feasible and outperforms approaches based on individual frames only. Detection accuracy may further improve with a larger dataset. Further improvements based on this approach may thus afford reliable automated detection in hospital and home settings in the future.

We chose to focus on detecting GTCSs because of their common occurrence, their clinical severity and secondary associated risks, including SUDEP. GTCSs are a well-established risk factor for SUDEP, and their timely detection and related early intervention may decrease the incidence of SUDEP [13]. GTCSs are also promising candidates for video-based

TABLE V
CHARACTERISTICS OF THE PATIENTS FOR NIGHT VIDEOS

Patient ID	Gender	Age at EEG [years]	Age at First Seizure [years]	Seizure Frequency/30d	Etiology	MRI Findings
1	female	9.0	1.0	22.5	genetic	malformation and delayed myelination
2	female	9.6	0.3	4.0	structural	infarction
3	male	12.0	7.0	0.0	unknown	encephalomalacia
4	female	22.0	2.0	4.0	unknown	normal
5	female	5.4	1.0	22.0	structure	malformation
6	female	6.0	6.0	5.0	unknown	normal
7	male	10.9	10.3	150.0	structure	malformation
8	male	13.3	1.5	NA	unknown	resection
9	female	5.5	0.7	NA	genetic	none
10	male	13.0	6.9	15.0	unknown	NA

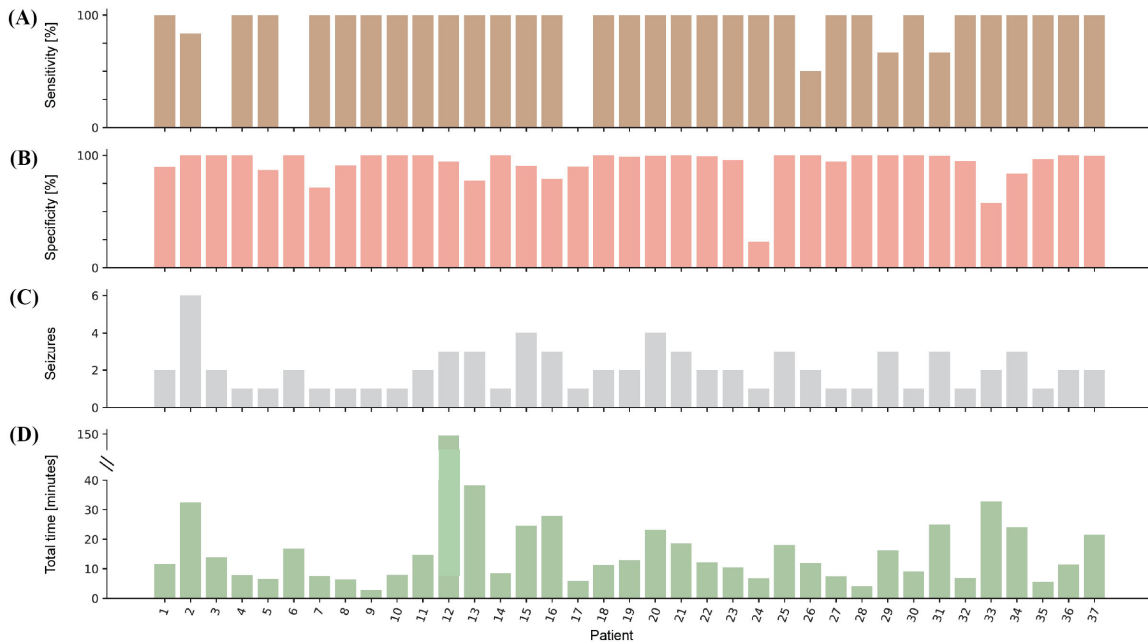


Fig. 2. Detection performance results. **A**, Sensitivity. **B**, Specificity. **C**, Number of seizures for each patient. **D**, Total duration of video data for each patient.

detection algorithms due to their characteristic motor manifestations, which may be captured by computer vision systems.

In our study, we combined CNN and LSTM deep learning algorithms because of their often-superior performance capabilities and the ability to classify video sequences without the need for specific feature engineering. Pretrained CNNs were first employed to extract spatial representations from individual video frames, and these representations were then fed into the LSTM network. LSTM architectures are capable of extracting distinct temporal representations. CNN+LSTM algorithms are end-to-end networks which do not require expert knowledge

or hand-crafted features of the particular context in which they are applied. They may thus directly infer motion patterns from videos, even when complex scenarios are encountered. In our case, for example, the seizure may occur far from the camera, or the motions of articulation may be complex during the seizures. These attributes make such an architecture desirable for a seizure detection approach. Also, the entire body can be analyzed simultaneously by the CNN+LSTM architecture, without the need for prior localization of the patient's position [11]. Once trained, inference with CNN+LSTM networks, as used here, is relatively fast. This is important to allow real-time video classification,

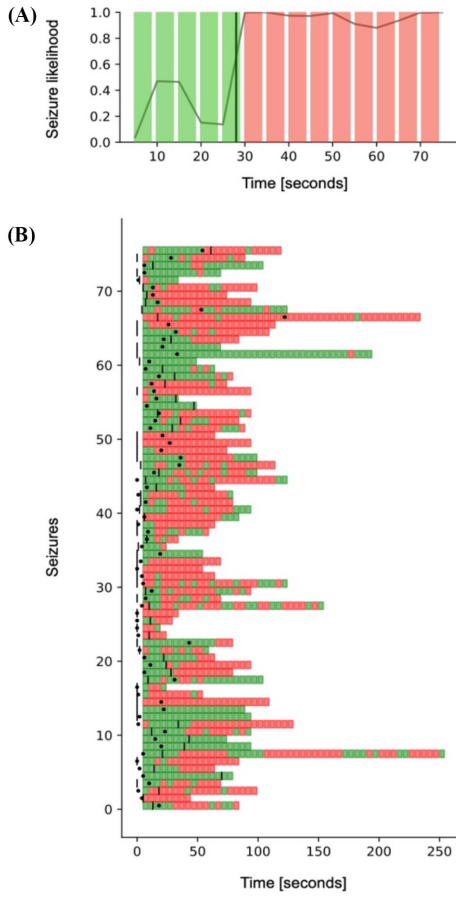


Fig. 3. Predicted seizure likelihood over the course of each seizure. **A**, Predicted seizure likelihood for one seizure. Likelihood is assessed every 5 seconds; if likelihood is smaller than 0.5 no seizure is detected (green), otherwise a seizure is detected during this 5-second epoch (red). **B**, Likelihood time course for all seizures. Black vertical lines indicate the first time another person aside from the patient is visible. Black round markers indicate the onset of the tonic phase.

which would be particularly relevant to alert caregivers, for example in the setting of an imminent SUDEP event.

For a seizure detection system to be useful it must not only be sensitive but also specific in order to avoid spurious false alarms [14]. Seizure detection based on EEG has been shown to be feasible with low energy consumption [34], [35], [36] while still achieving high sensitivity and low FDR results as well as detection delays of about 13 seconds [37], thus being comparable to our results, as pertaining to generalized tonic-clonic seizures. Here we report sensitivity, specificity and detection latency derived from a LOSO-CV approach, which allows for an unbiased estimation of the true generalization error by evaluating subject-to-subject variation. This approach guarantees that the training does not underpin training for an individual but for a group dataset – and as such, the performance is more reliable and generalizable. Our results show that the video-based GTCS detection system is encouraging in terms of overall performance, but also requires further improvement to be clinically useful. These performance values are superior to some previous video-based detection systems for neonatal

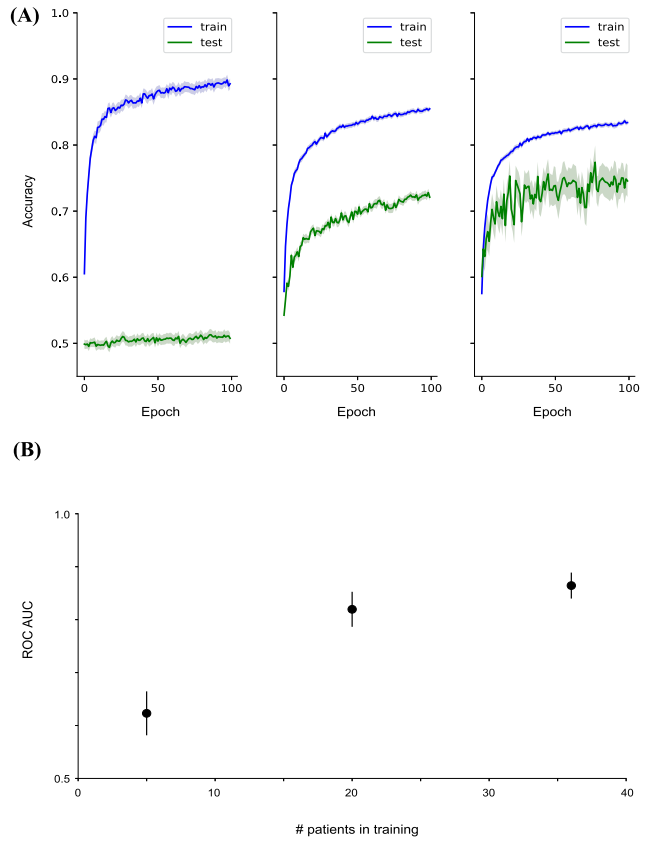


Fig. 4. Improvement of detection performance as a function of size of training data. **A**, Learning curves for training on 5 (left), 20 (middle) and 36 (right) patients and testing on one patient. **B**, The corresponding AUC values. Whiskers and shaded error markers denote standard error of the mean (s.e.m.).

clonic seizure (sensitivity of 48–86%, specificity of 67–89%) [6] or nocturnal myoclonic seizures (sensitivity of 74%) [15]. Focusing on convulsive seizures, one study recently reported an outstanding sensitivity of 100% and a low false positive rate using a hand-crafted detection algorithm [16]. In this setting, a detection latency of ≤ 10 seconds was achieved in 78% of patients with convulsive seizures. In contrast to our approach, which included data from sleeping and awake patients pursuing different kinds of activities, however, these studies only focused on nocturnal seizures which may be one explanation for the stronger performance reported therein. Furthermore, we here studied a pediatric patient population, and pediatric GTCSs are often not as stereotyped and may thus be harder to detect in comparison. Only very few studies have previously explored deep learning for video seizure detection. One video-based study explored detection using gated recurrent unit (GRU) networks [17]. However, it is not clear which seizure types were considered for analysis in this study, making a direct comparison to our results based on GTCSs difficult. More generally, our work highlights that it is crucial to include long and variable data both for training and testing. While it may be important to report the general feasibility of an approach using only relatively short data segments, e.g., for the detection of seizures based on individual

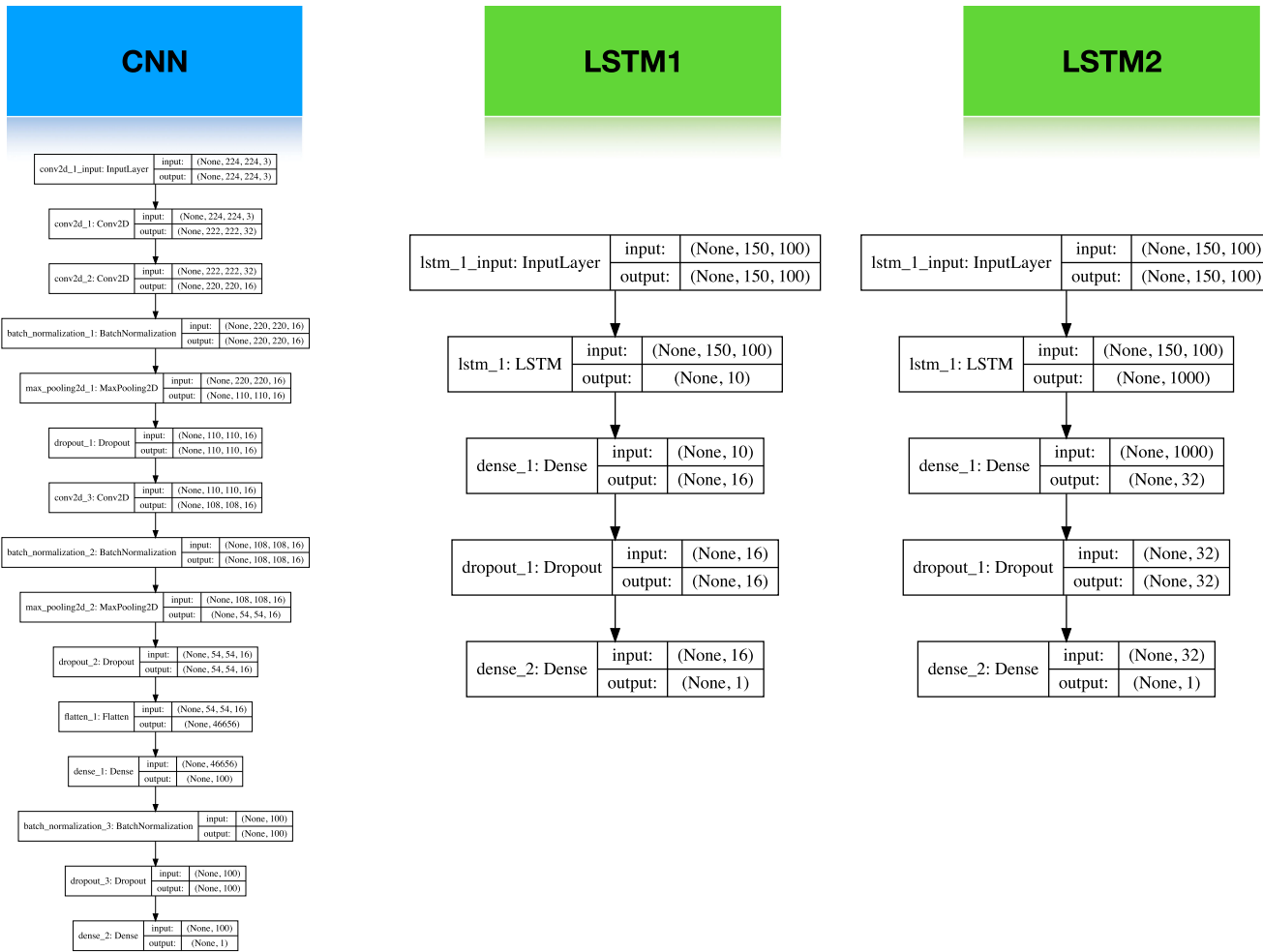


Fig. 5. Network architectures. When the CNN was combined with LSTM networks, the top layer was removed yielding a 100-element long vector which was then fed into the LSTM network. To train the CNN network, learning rate was set to 0.001, batch size to 32, Adam optimizer, 150 epochs. To train LSTM networks, learning rate was set to 0.01, batch size to 32, Adam optimizer, 100 epochs.

video frames or on video sequences, the true performance and clinical relevance of an approach can only be assessed on longer data samples that capture variability under realistic conditions, as attempted in our study. Higher variability in our data may thus explain the relatively high FDR in comparison to other studies, yet provide a more realistic real-life application of these methods. While this relatively high FDR requires further improvement to become a viable real-time closed loop warning system for home use, it is already a functional detection system as it flags suspicious video segments that can subsequently be reviewed by nurses, technicians, or clinicians more rapidly.

From a user-perspective, detection latency is another important characteristic of any detection algorithm. If seizures are detected only a few seconds after onset, then chances for a timely warning to caregivers and respective earlier treatment increase [14]. In this study, we assessed the latency based on clinical onset; of note, typical convulsions are often not present at the onset. A recent study reported detection latency (≤ 10 seconds) in 78% of convulsive patients with use of an automatic segmentation detection system that was based on optical flow [16]. Another study reported shorter detection latency (3.41 seconds) of a

detection system based on video and deep learning [17]; however, details regarding the population or seizure types are not fully available, making the comparison to our specific pediatric GTCS detection results under real-life monitoring conditions difficult. Finally, our approach differs from a commercially available nocturnal movement monitor (SAMi) [18], which was developed for detection of abnormal movements during sleep. This device is designed to be used at night and to detect abnormal movements that continue for at least 15 seconds. In contrast, the detection system we introduce here was trained on data from day and night video monitoring, including patients lying in bed or being awake, engaging in various activities, and it is specifically targeted at GTCS detection with relatively low detection latency, therefore potentially providing fewer false positive detections.

During inpatient seizure videos, caretakers and family members are frequently approaching the bed and the patient, which may impact the performance of a detection algorithm, or potentially influencing seizure identification criteria. In control analyses adjusting for potential confounding by other persons in the seizure video, we found that ten seizures were detected without any other people appearing in the videos. These results

suggest that the proposed video seizure detection works with and without other people in the video, thus ruling out sole seizure detection based on the presence of other people in the video.

The performance of the detection system could also be influenced by other factors, including occlusion by a blanket, illumination changes and interaction with other people [19]. In our study, the proportion of occlusion, illumination, other people appearing in the videos, wakefulness, different resolution of the original video, and interaction with other people were not significantly different between the shorter and longer detection latency groups. Therefore, these factors may not have obvious effects on detection latencies in our study. Furthermore, the functionality of our system may not be impaired under conditions of normal home or in-hospital settings when the patient is typically alone. Other factors, including the distance between the patients and camera or resolution changes of video data may potentially influence the performance of the model. While regression analysis may further untangle the potential effects of these various variables in future studies, the current findings suggest that our GTCS detection system may overcome some limitations of previous approaches.

Results need to be interpreted in the setting of data acquisition. In this study, we aimed to use video data “as is” in an attempt to most closely capture real-life conditions. To retain the natural condition of the patient and use as much data as possible, we thus also included several ictal videos with patients covered by a blanket throughout the occurrence of the seizure. As such, some of the seizures were subtle and not easy to detect, even from a perspective of a trained human looking for GTCS. Inclusion of these videos along with the high variability of patient positions and actions associated with daytime videos may have contributed to detection rates slightly less than 90%. In addition, the inclusion of the patients was not random and inclusion of multiple seizures by the same patient may have contributed to selection bias. While the goal of the current study was to generally assess the feasibility of deep learning based GTCS seizure detection algorithm and compare it to detection based on individual video frames, detection performance will require further improvement and validation in future prospective, long-term studies. Deep learning generally benefits from large datasets. This has also been demonstrated in the current study as well as in other detection and forecasting applications related to epilepsy [20]. Thus, it is conceivable that additional data will help improve our detection algorithm further, taking into account variability seen in the videos and other variables, such as changes in camera position, among others. Future methods may potentially benefit from hybrid approaches including feature extraction or model-based image pre-processing in order to address variability. Lastly, our detection system was solely based on video. Real-life data may offer additional modalities, such as sound, among others. Integrating additional data, such as audio along with other multimodal data streams, such as EEG [32], [40], presumably may lead to further improvements in detection performance.

Our approach to recognizing seizures in video recordings resembles some similarity to other work on human activity

recognition (HAR), a field of extensive study with successful applications including home behavior analysis [21], video surveillance [22], gait analysis [23], and gesture recognition [24]. HAR has also greatly benefited from deep learning [25]. In principle, seizure detection may also benefit from using methods like DeepPose [26]. The partial covering of body parts as seen in our videos along with the high variability of semiology phenotypes and the limited data availability relative to other applications of DeepPose, however, may pose some limitations to this approach and will need to be assessed.

V. CONCLUSION

Automated video-based GTCS detection based on deep learning is feasible and efficacious, with good performance (mean sensitivity: 88%, mean specificity: 92%, average detection latency after presumed clinical seizure onset: 22 s). This approach may overcome some limitations associated with more traditional methods, may serve as a benchmark for future analyses, and may improve further with larger datasets and multi-modal data streams.

CONFLICT OF INTEREST

TL and CM disclose a pending intellectual property filing related to video seizure detection through Boston Children’s Hospital. TL serves on the Council of the American Clinical Neurophysiology Society, as founder and consortium PI of the pediatric status epilepticus research group (pSERG), as an Associate Editor for Wyllie’s Treatment of Epilepsy 6th edition and 7th editions, and as a member of the NORSE Institute, and CCEMRC. He served as Associate Editor of Seizure, and served on the Laboratory Accreditation Board for Long Term (Epilepsy and Intensive Care Unit) Monitoring in the past. He is part of patent applications to detect and predict clinical outcomes, and to detect, manage, diagnose, and treat neurological conditions, epilepsy, and seizures. Dr. Loddenkemper is co-inventor of the TriVox Health technology, and Dr. Loddenkemper, and Boston Children’s Hospital might receive financial benefits from this technology in the form of compensation in the future. He received research support from the Epilepsy Research Fund, NIH, the Epilepsy Foundation of America, the Epilepsy Therapy Project, the Pediatric Epilepsy Research Foundation, and received research grants from Lundbeck, Eisai, Upsher-Smith, Mallinckrodt, Sunovion, Sage, Empatica, and Pfizer, including past device donations from various companies, including Empatica, SmartWatch, and Neuro-electrics. He performs video electroencephalogram long-term and ICU monitoring, electroencephalograms, and other electrophysiological studies at Boston Children’s Hospital and affiliated hospitals and bills for these procedures and he evaluates pediatric neurology patients and bills for clinical care. He has received speaker honorariums/travel support from national societies including the AAN, AES and ACNS, and for grand rounds at various academic centers. His wife, Dr. Karen Stannard, is a pediatric neurologist and she performs video electroencephalogram long-term and ICU monitoring, electroencephalograms, and other electrophysiological studies and bills for these procedures and

she evaluates pediatric neurology patients and bills for clinical care. None of the other authors has any conflict of interest to disclose. We confirm that we have read the Journal's position on issues involved in ethical publication and affirm that this report is consistent with those guidelines.

REFERENCES

- [1] T. Tomson, T. Walczak, M. Sillanpaa, and J. W. Sander, "Sudden unexpected death in epilepsy: A review of incidence and risk factors," *Epilepsia*, vol. 46, no. 11, pp. 54–61, 2005.
- [2] N. B. Karayannidis *et al.*, "Computerized motion analysis of videotaped neonatal seizures of epileptic origin," *Epilepsia*, vol. 46, no. 6, pp. 901–917, Jun. 2005.
- [3] N. B. Karayannidis, G. Tao, J. D. Frost Jr., M. S. Wise, R. A. Hrachovy, and E. M. Mizrahi, "Automated detection of videotaped neonatal seizures based on motion segmentation methods," *Clin. Neurophysiol.*, vol. 117, no. 7, pp. 1585–1594, Jul. 2006.
- [4] N. B. Karayannidis, Y. Xiong, J. D. Frost, Jr., M. S. Wise, R. A. Hrachovy, and E. M. Mizrahi, "Automated detection of videotaped neonatal seizures based on motion tracking methods," *J. Clin. Neurophysiol.*, vol. 23, no. 6, pp. 521–531, Dec. 2006.
- [5] G. M. Ntonfo, G. Ferrari, R. Raheli, and F. Pisani, "Low-complexity image processing for real-time detection of neonatal clonic seizures," *IEEE Trans. Inf. Technol. Biomed.*, vol. 16, no. 3, pp. 375–382, May 2012.
- [6] F. Pisani *et al.*, "Real-time automated detection of clonic seizures in newborns," *Clin. Neurophysiol.*, vol. 125, no. 8, pp. 1533–1540, Aug. 2014.
- [7] S. Kalitzin, G. Petkov, D. Velis, B. Vledder, and F. Lopes da Silva, "Automatic segmentation of episodes containing epileptic clonic seizures in video sequences," *IEEE Trans. Biomed. Eng.*, vol. 59, no. 12, pp. 3379–3385, Dec. 2012.
- [8] D. Ahmedt-Aristizabal, C. Fookes, S. Dionisio, K. Nguyen, J. P. S. Cunha, and S. Sridharan, "Automated analysis of seizure semiology and brain electrical activity in presurgery evaluation of epilepsy: A focused survey," *Epilepsia*, vol. 58, no. 11, pp. 1817–1831, Nov. 2017.
- [9] F. Achilles, F. Tombari, V. Belagiannis, A. M. Loesch, S. Noachtar, and N. Navab, "Convolutional neural networks for real-time epileptic seizure detection," *Comput. Methods Biomech. Biomed. Eng.: Imag. Visual. Article*, vol. 6, no. 3, pp. 264–269, 2018.
- [10] D. Ahmedt-Aristizabal, C. Fookes, K. Nguyen, S. Denman, S. Sridharan, and S. Dionisio, "Deep facial analysis: A new phase i epilepsy evaluation using computer vision," *Epilepsy Behav.*, vol. 82, pp. 17–24, May 2018.
- [11] D. Ahmedt-Aristizabal, S. Denman, K. Nguyen, S. Sridharan, S. Dionisio, and C. Fookes, "Understanding patients' behavior: Vision-based analysis of seizure disorders," *IEEE J. Biomed. Health Inform.*, vol. 23, no. 6, pp. 2583–2591, Nov. 2019.
- [12] D. Ahmedt-Aristizabal, C. Fookes, S. Denman, K. Nguyen, S. Sridharan, and S. Dionisio, "Aberrant epileptic seizure identification: A computer vision perspective," *Seizure*, vol. 65, pp. 65–71, Feb. 2019.
- [13] L. Vilella *et al.*, "Postconvulsive central apnea as a biomarker for sudden unexpected death in epilepsy (SUDEP)," *Neurology*, vol. 92, no. 3, pp. e171–e182, Jan. 15, 2019.
- [14] F. Mormann, R. G. Andrzejak, C. E. Elger, and K. Lehnertz, "Seizure prediction: The long and winding road," *Brain*, vol. 130, no. Pt 2, pp. 314–333, Feb. 2007.
- [15] K. Cuppens *et al.*, "Using spatio-temporal interest points (STIP) for myoclonic jerk detection in nocturnal video," *Conf. Proc. IEEE Eng. Med. Biol. Soc.*, vol. 2012, pp. 4454–4457, 2012.
- [16] E. E. Geertsema *et al.*, "Automated video-based detection of nocturnal convulsive seizures in a residential care setting," *Epilepsia*, vol. 59, no. 1, pp. 53–60, Jun. 2018.
- [17] Z. Fang, H. Leung, and C. S. Choy, and Ieee, "Spatial temporal gru convnets for vision-based real time epileptic seizure detection," in *Proc. IEEE 15th Int. Symp. Biomed. Imag.*, 2018, pp. 1026–1029.
- [18] "SAMi - the sleep activity monitor," ed: <https://www.samialert.com>, 2020.
- [19] M. Pedadidis, M. Tsiknakis, and N. Leitgeb, "Vision-based motion detection, analysis and recognition of epileptic seizures—A systematic review," *Comput. Methods Programs Biomed.*, vol. 108, no. 3, pp. 1133–1148, Dec. 2012.
- [20] C. Meisel *et al.*, "Machine learning from wristband sensor data for wearable, non-invasive seizure forecasting," *Epilepsia*, vol. 61, pp. 2653–2666, Dec. 2020.
- [21] P. Vepakomma *et al.*, "A-wristocracy: Deep learning on wrist-worn sensing for recognition of user complex activities," in *Proc. IEEE 12th Int. Conf. Wearable Implantable Body Sensor Netw.*, 2015, pp. 1–6.
- [22] J. Qin, L. Liu, Z. Zhang, Y. Wang, and L. Shao, "Compressive sequential learning for action similarity labeling," *IEEE Trans. Image Process.*, vol. 25, no. 2, pp. 756–769, Feb. 2016.
- [23] N. Hammerla, S. Halloran, and T. Ploetz, "Deep, convolutional, and recurrent models for human activity recognition using wearables," in *Proc. Int. Joint Conf. Artif. Intell.*, 2016, pp. 1533–1540.
- [24] Y. Kim and B. Toomajian, "Hand gesture recognition using micro-doppler signatures with convolutional neural network," *IEEE Access*, 2016.
- [25] J. Wang *et al.*, "Deep learning for sensor-based activity recognition: A survey," *Pattern Recognit. Lett.*, vol. 119, pp. 3–11, 2019.
- [26] A. Toshev and C. Szegedy, "DeepPose: Human pose estimation via deep neural networks," in *Proc. IEEE Conf. Comput. Vis. Pattern Recognit.*, 2014, pp. 1653–1660.
- [27] Y. Roy, H. Banville, I. Albuquerque, A. Gramfort, T. H. Falk, and J. Faubert, "Deep learning-based electroencephalography analysis: A systematic review," *J. Neural Eng.*, vol. 16, Aug. 14, 2019, Art. no. 051001.
- [28] S. Beniczky and J. Jeppesen, "Non-electroencephalography-based seizure detection," in *Proc. Curr. Opin. Neurol.*, pp. 198–204, 2019.
- [29] S. Kusmakar, C. Karmakar, B. Yan, T. Obrien, R. Muthuganapathy, and M. Palaniswami, "Automated detection of convulsive seizures using a wearable accelerometer device," *IEEE Trans. Biomed. Eng.*, vol. 66, pp. 421–432, Feb. 2019.
- [30] M. Z. Poh, T. Loddenkemper, N. C. Swenson, S. Goyal, J. R. Madsen, and R. W. Picard, "Continuous monitoring of electrodermal activity during epileptic seizures using a wearable sensor," *Conf. Proc. IEEE Eng. Med. Biol. Soc.*, vol. 2010, pp. 4415–4418, 2010.
- [31] C. A. Szabo *et al.*, "Electromyography-based seizure detector: Preliminary results comparing a generalized tonic-clonic seizure detection algorithm to video-EEG recordings," *Epilepsia*, vol. 56, pp. 1432–1437, Sep. 2015.
- [32] M. Khan *et al.*, "A low complexity patient-specific threshold based accelerator for the grand-mal seizure disorder," in *Proc. IEEE Biomed. Circuits Syst.*, Oct. 2017, pp. 348–351.
- [33] S. Kalitzin, G. Petkov, D. Velis, B. Vledder, and F. Lopes da Silva, "Automatic segmentation of episodes containing epileptic clonic seizures in video sequences," *IEEE Trans. Biomed. Eng.*, vol. 59, no. 12, pp. 3379–3385, 2012.
- [34] M. Altaf and J. Yoo, "A 1.83 μ J/Classification, 8-Channel patient-specific epileptic seizure classification SoC using non-linear support vector machine," *IEEE Trans. Biomed. Circ. Syst.*, vol. 10, no. 1, pp. 49–60, Feb. 2016.
- [35] M. Mirzaei, M. Salam, D. Nguyen, and M. Sawan, "A fully-asynchronous low-power implantable seizure detector for self-triggering treatment," *IEEE Trans. Biomed. Circuits Syst.*, vol. 7, no. 5, pp. 563–572, Oct. 2013.
- [36] K. Abdelhalim, V. Smolyakov, and R. Genov, "Phase-Synchronization early epileptic seizure detector VLSI architecture," *IEEE Trans. Biomed. Circuits Syst. Vol.*, vol. 5, no. 5, pp. 430–438, Oct. 2011.
- [37] M. Salam *et al.*, "A novel low-power-implantable epileptic seizure-onset detector," *IEEE Trans. Biomed. Circuits Syst.*, vol. 5, no. 6, pp. 568–578, Dec. 2011.
- [38] C. Meisel and T. Loddenkemper, "Seizure prediction and intervention," *Neuropharmacology*, vol. 172, 2020, Art. no. 107898.
- [39] C. Ufongene, R. E.. Atrache, T. Loddenkemper, and C. Meisel, "Electrocardiographic changes associated with epilepsy beyond heart rate and their utilization in future seizure detection and forecasting methods," *Clin. Neurophysiol.*, vol. 131, pp. 866–879, 2020.
- [40] C. Meisel and K. Bailey, "Identifying signal-dependent information about the preictal state: A comparison across ECoG, EEG and EKG using deep learning," *Lancet EBioMed.*, vol. 45, pp. 422–431, 2019.